Project No: 603502

DACCIWA

"Dynamics-aerosol-chemistry-cloud interactions in West Africa"

Deliverable

D6.6 Satellite evaluation

Due date of deliverable:	30/11/2018
Completion date of deliverable:	**17**/12/2018
Start date of DACCIWA project:	1st December 2013 **Project duration:** 60 months
Version:	[V1.0]
File name:	[D6.6_Satallite_evaluation_DACCIWA_v1.0.pdf]
Work Package Number:	**6**
Task Number:	**6**
Responsible partner for deliverable:	**KNUST**
Contributing partners:	**KIT**
Project coordinator name:	Prof. Dr. Peter Knippertz
Project coordinator organisation name:	Karlsruher Institut für Technologie

The DACCIWA Project is funded by the European Union's Seventh Framework Programme for research, technological development and demonstration under grant agreement no 603502.

Dissemination level		
PU	Public	**x**
PP	Restricted to other programme participants (including the Commission Services)	
RE	Restricted to a group specified by the consortium (including the Commission Services)	
CO	Confidential, only for members of the consortium (including the Commission Services)	

Nature of Deliverable		
R	Report	
P	Prototype	
D	Demonstrator	
O	Other	**x**

DOCUMENT INFO

Authors

Author	Beneficiary Short Name	E-Mail
Leonard K. Amekudzi	KNUST	Leonard.amekudzi@gmail.com
Winifred A. Atiah	KNUST	Winifred.a.atiah@aims-senegal.org
Andreas H. Fink	KIT	andreas.fink@kit.edu
Marlon Maranan	KIT	marlon.maranan@kit.edu

Changes with respect to the DoW

Issue	Comments

Dissemination and uptake

Target group addressed	Project internal / external
Scientific	Internal and external

Document Control

Document version #	Date	Changes Made/Comments
V0.1	24.10.2018	Template with basic structure
V0.2	29.11.2018	Version for approval by the General Assembly
V1.0	17.12.2018	Final version approved by the General Assembly with final corrections

Table of Contents

1 Introduction

Rainfall plays a crucial role in the socio-economic development of the African continent, particularly in those countries where agriculture is predominantly rain-fed. The availability of good drinking water, food and energy supplies in the continent is largely dependent on rainfall. Rainfall is reported as one of the key determinants of the poor socio-economic state of the continent (Barrios et al., 2010). In Ghana, rainfall has a great is impact on the general food production of the region as it determines the time and type of crops to grow (Yengoh et al., 2010). Therefore, rainfall variability in the region poses serious economic risks to the country. However, our understanding of the processes involved in rainfall variability and extremes are limited and this is partly attributable to the lack of dense gauge networks in the region. This therefore has augmented the use of surrogates as substitutes or complements to the existing ground-based measurements (Dezfuli et al., 2017). In recent times, efforts have been made to increase the number of rain gauge networks recording rainfall at high temporal resolution while extending the satellite-based rainfall products to higher spatio-temporal scales for their applicability within the continent.

The Dynamic-Aerosol-Chemistry-Cloud Interactions in West Africa (DACCIWA) rain gauge network is a typical, yet in the region hitherto unique example of such gauge networks. Within the DACCIWA project, seventeen optical rain gauges have been installed in the Ashanti region of Ghana in 2015 (see Figure 1 and Deliverable D6.3). The DACCIWA optical rain gauges (DOGs) records rainfall data on a minute temporal resolution. The high temporal and spatial in-situ sampling of rainfall events allows for the validation of a relatively new gauge-calibrated satellite rainfall product: The GPM IMERG (Global Precipitation Mission, Integrated Multi-satellite Retrievals for GPM) product (Huffman et al., 2015b) provides half-hourly gridded rainfall estimates between 60°N and 60°S since 2014 at a grid-spacing of 0.1°. Compared to the successful and widely used predecessor, the Tropical Rainfall Measuring Mission (TRMM) Multi-satellite Precipitation Analysis (TMPA, Huffman et al., 2007) product, the temporal and spatial resolution has been increased by a factor of six and 2.5, respectively. Building upon the quality-controlled, one-minute-based rainfall dataset of the Kumasi rain gauge network (Maranan et al., 2018), which was described in deliverable D6.3, the increased spatiotemporal resolution of IMERG enables us to investigate its performance even on a timescale of short-duration rainfall events on the order of tens of minutes. The following section compares the rainfall estimates by the DACCIWA optical rain gauge network and IMERG and puts them into the context of the seasonal cycle of rainfall of the West African monsoon.

2 Validation of GPM at daily time scales

2.1 Statistical validation

The latest version of GPM IMERG (V5) was inter-compared with the observations from the DOGs at nine stations. For these nine stations, also daily data (09 – 09 UTC) from a co-located GMET (Ghana Meteorological Agency) manual rain gauge were available for 2016-2017. The nine stations were selected since the comparison between daily rainfall from DOG and GMET gauges lend confidence on the performance of the DACCIWA gauges (cf. Deliverable 6.3 and Table 1 and Fig. 1 therein for meta-information and the location, respectively, of the nine stations). The validation of GPM IMERG was conducted by creating Taylor (Fig. 1) and error diagrams (i.e. Bias vs. Centred Root Mean Square Error (CRMSE) errors, Fig. 2) for the four seasons December-February (DJF, dry season), March-May (MAM, first rainy season), June-August (JJA, includes little dry season) and September-November (SON, second rainy season) of the years 2016 and 2017. From Fig. 1, the Pearson correlation values r for all but the Nsuta, Mankranso and Bompata stations are larger than 0.5 in the DJF dry season. The standard deviation of IMERG at the Agromet and Jamasi stations were closest to that of observations, thus GPM IMERG captures the day-to-day variability at these stations

comparatively well. These stations also have a high correlation and low CRMSE in the dry season. During the first rainy season (MAM), GPM IMERG in all but the Mankranso, Jamasi and Bompata stations was observed to correlate well with DOGs with r values >=0.5. GPM IMERG in the Bekwai and Akrokeri stations is observed to mimic gauge relatively better with high r values and similar standard deviations to that of DOGs (Fig. 1). GPM IMERG in all stations had small bias values (<2mm/day) although CRMSE in the Jamasi station was relatively high (18mm/day, Fig. 2). IMERG correlated well with the DOGs during the JJA seasons compared to other seasons as almost all stations but the Mankranso station recorded high r values (Fig. 1). The rainfall variability in this season was also relatively well captured by IMERG in the Mampong, Ejura and Nsuta stations. Bias values are relatively minimal compared to other seasons (bias <= 1mm/day, Fig. 2). IMERG generally performs poorer in the SON season as the values for the correlation coefficient r at all stations but in Bekwai and Mapong were < 0.5 (Fig. 1). Bias values in all stations were less than 2mm/day, except for Mankranso in the dry season (Fig. 2).

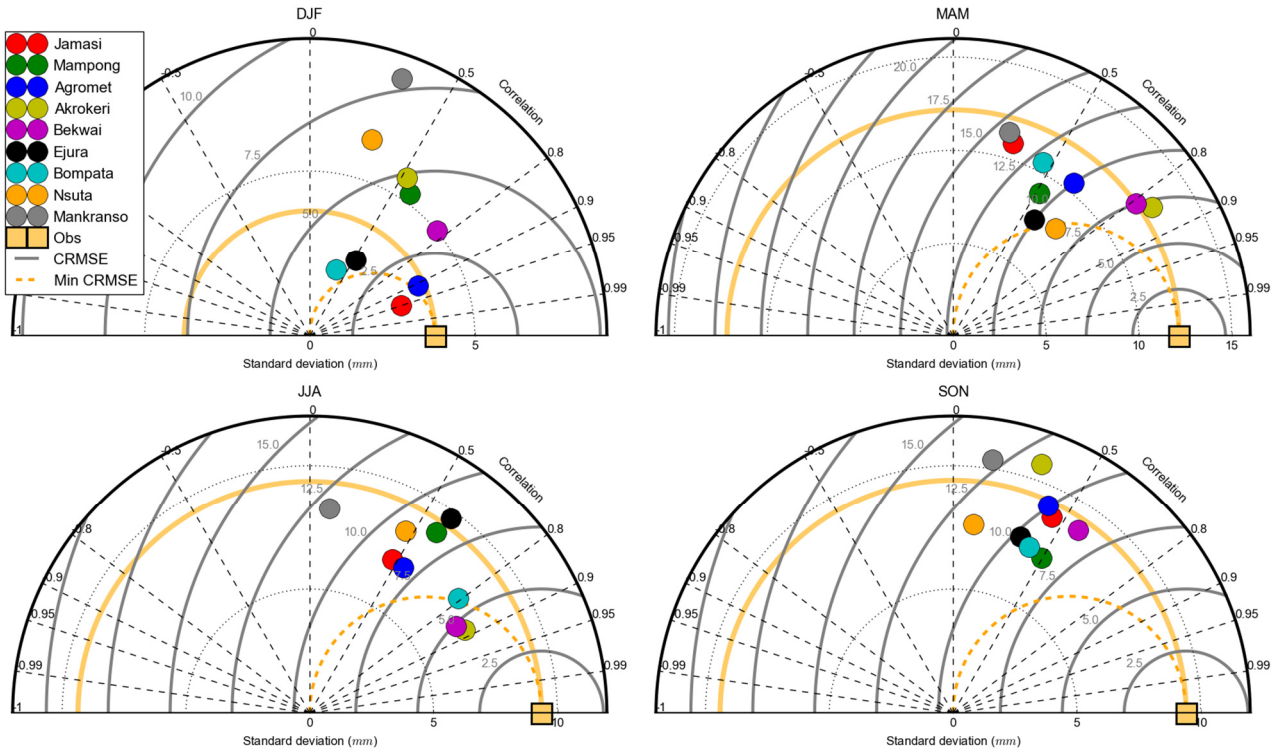

Figure 1: *Taylor diagrams summarising the performance of IMERG relative to DOGs at the co-located nine stations (see inset in top left panel) during DJF, MAM, JJA and SON seasons of 2016-2017.*

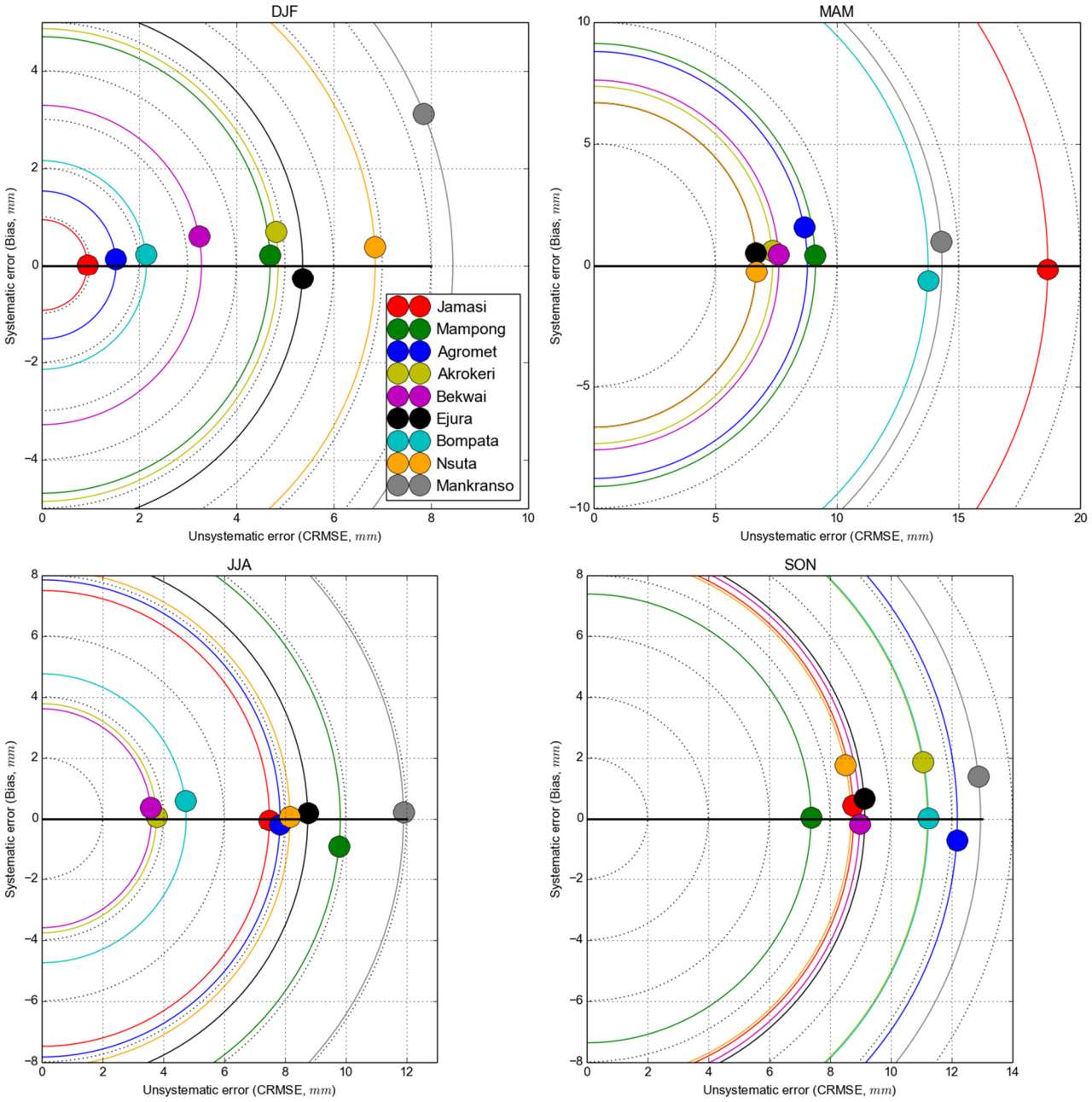

Figure 2: *Error diagrams summarising the performance of IMERG relative DOGs at the co-located stations during DJF, MAM, JJA and SON seasons of 2016-2017.*

It is interesting to compare the new GPM IMERG product against its predecessor product TRMM. The former product relies on a dual-frequency, active space-born radar aboard the GPM Core Observatory launched in early 2014 (Hou et al. 2014), whereas the TRMM satellite had a single-frequency radar only. This allows a more detailed determination of the size distribution of precipitation particles in IMERG. Thus it is tempting to assume that the GPM IMERG product is superior to the TRMM product. As can be seen in Figs. 3 and 4 that correspond to Figs. 1 and 2, GPM IMERG precipitation estimates are indeed better than TRMM, except in the SON season when improvements are not evident in the diagrams. An interpretation of the relatively poor performance of the products in the second rainy season (SON) is not obvious, but may be related to less organized rainfall from warmer clouds (Maranan et al. 2018).

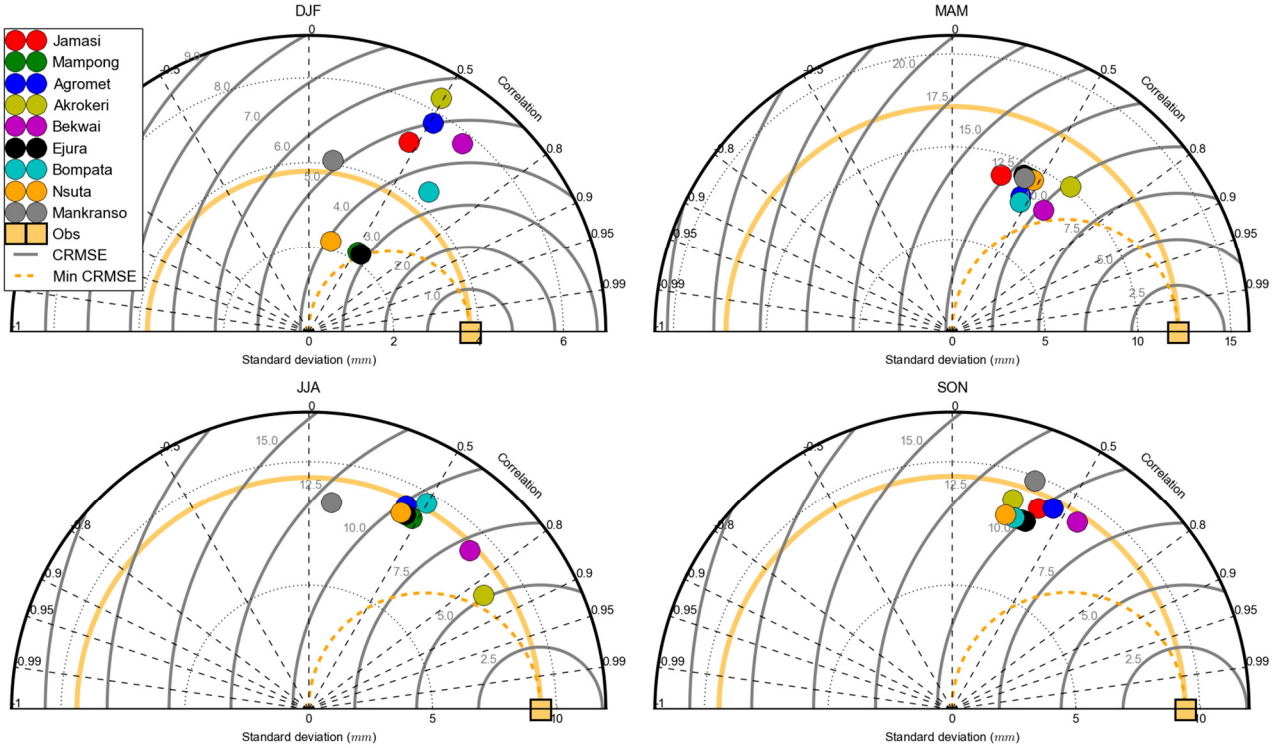

Figure 3: *Taylor diagram summarising the performance of TRMM relative DOGs at the co-located stations during DJF, MAM, JJA and SON seasons of 2016-2017.*

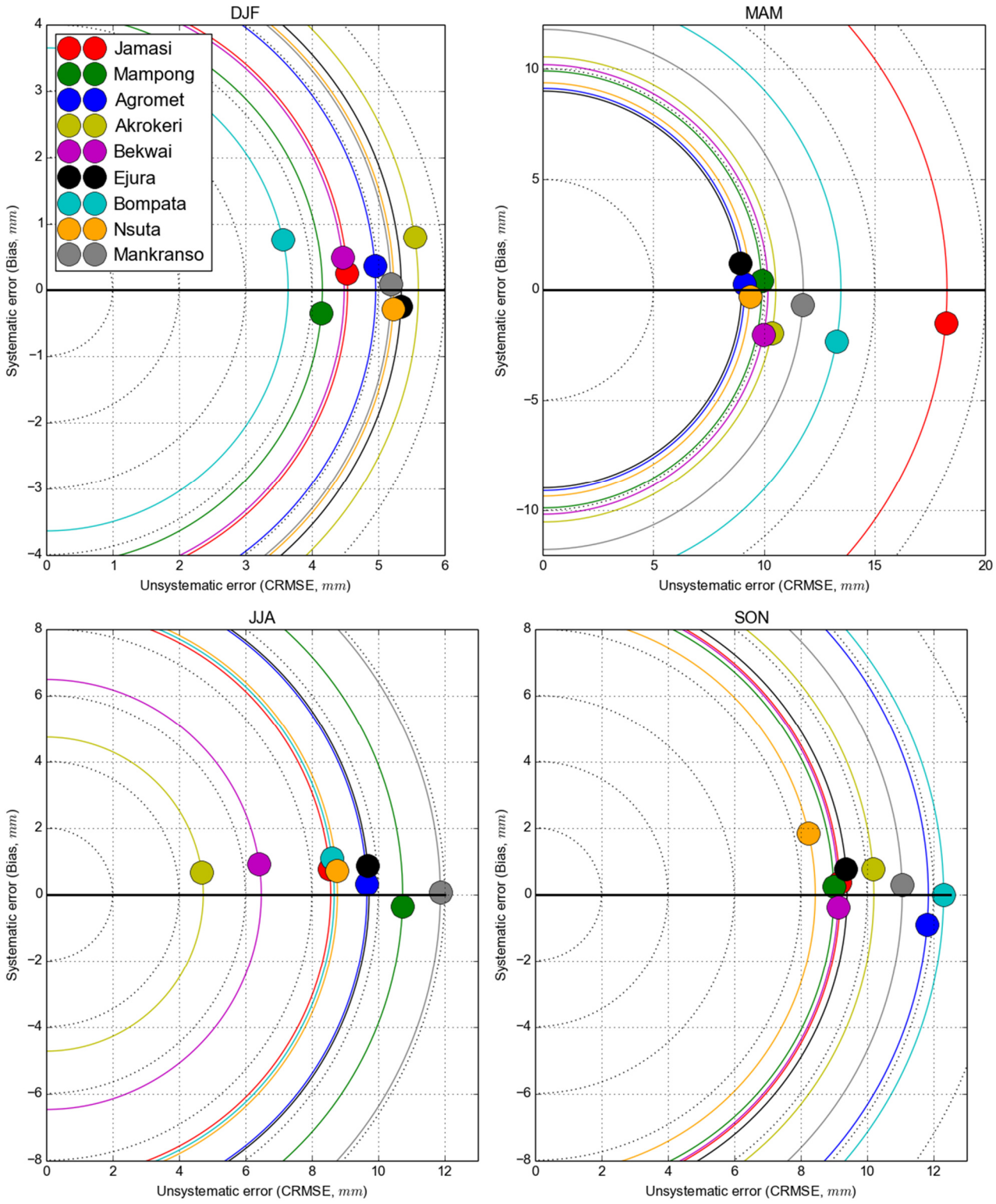

Figure 4: *Error diagram summarising the performance of IMERG relative DOGs at the co-located stations during DJF, MAM, JJA and SON seasons of 2016-2017.*

2.2 Validation based on different types of rainfall

Before GPM IMERG itself is evaluated, we defined different rainfall types within the rain gauge dataset in order to analyse different rainfall situations. Across all rain gauges, rainfall signals may emerge from the same precipitating cloud structure with a certain time lag, depending on their relative distance to each other. The correlation-regression method described by Upton (2002) was used to identify and assign these events. Each event is presented as a single dot in Fig. 5. Here, the rainfall type is defined with respect to the duration and mean rainfall rate of the event. While we distinguish between “short rainfall” (SR, all blueish dots) and “long rainfall” (LR, all reddish dots), the intensity definition ranges from “weak” over “strong” to “intense”. Accordingly, a “weak short rainfall” event, for example, is called “WSR” (see figure caption for more details). An in-depth analysis of the specific rainfall profiles of each rainfall category reveals that LR can be typically considered as being related to Mesoscale Convective Systems (MCSs) of different intensities, where the long duration is caused by the trailing stratiform part (not shown, cf. Fink et al., 2006). Some of the intense short rainfall (ISR) may also be considered as MCSs, particularly in an early stage without a pronounced stratiform part. Considering the indicated relative frequency and contribution to total rainfall in Fig. 5 (%n and %RR, respectively), it becomes apparent that SR dominates rain event population over the rain gauge domain with around 90%, but contribute only 40% to the total rainfall. A satellite-based study about the importance of different rainfall types over southern West Africa by Maranan et al. (2018) comes to a similar conclusion that MCSs account for the majority of total rainfall despite being strongly outnumbered by less intense rainfall systems.

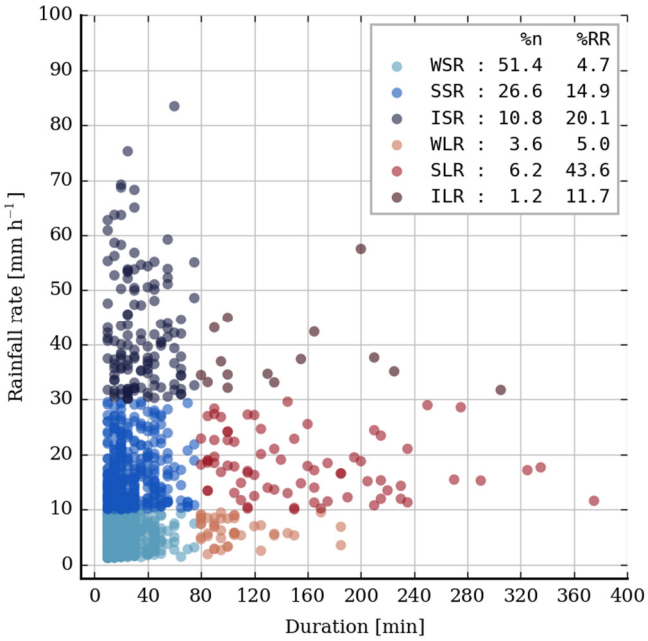

Figure 5: *Rainfall events identified within the rain gauge dataset and plotted with respect to the event duration (abscissa) and mean rainfall rate (ordinate). The latter was calculated by dividing the total rainfall amount of the event by its duration. The blue dots refer to “short rainfall events (SR)” (< 80 minutes), the different shades of blue refer to different mean rainfall intensities, from “weak” (W, light blue) over “strong” (S, medium blue) to “intense” (I, dark blue). Accordingly, a “weak short rainfall” event, for instance, is abbreviated “WSR”. The red shadings refer to “long rainfall (LR)” (>= 80 minutes), the nomenclature and colour shadings for the intensities are the same for SR. In the inset rectangle, the relative frequency (%n) and its contribution to total rainfall (%RR) are indicated for all rainfall types.*

The rainfall totals of the rainfall types from the perspective of the seasonal cycle are shown in Fig. 6, separately for quality-controlled DACCIWA rain gauge data for 2016 and 2017. First of all, the rain gauge domain encountered different seasonal cycles between 2016 and 2017, with the former year exhibiting a weak primary rainy season between April and June compared to the usually weaker secondary rainy period in September and October (see solid white curve in Fig. 6a). The situation was reversed in 2017 (Fig. 6b). The coloured bars, which show the monthly relative contribution of the defined rainfall types, indicate that LRs (all red bars) generally dominate the rainfall contribution from April to October. In the dry season from November to February, the large fraction from SRs (all blue bars) suggests a decreased activity of MCSs, which is consistent with long-term satellite observations (e.g. Maranan et al., 2018). The associated curves of mean monthly rainfall for IMERG (solid green line) show good accordance with the rain gauges. IMERG is able to capture the characteristics of the different seasonal cycles of 2016 and 2017 well, which has already been discussed in Section 2.1. It shall be noted, however, that like the TRMM predecessor product, IMERG precipitation rates are calibrated by the monthly Global Precipitation Climatology Centre (GPCC) gauge-only product (Huffman et al., 2015a). Thus, the agreement at monthly time scales does not come as a surprise, since gauge data were used in GPCC during the 2016 and 2017 seasons. The questions that will be addressed in the following are:

- How well does IMERG perform on a daily basis?
- How well are the different rainfall types on a sub-daily basis captured in IMERG?
- Based on the previous question, how does this translate into a seasonal perspective like Fig. 6?

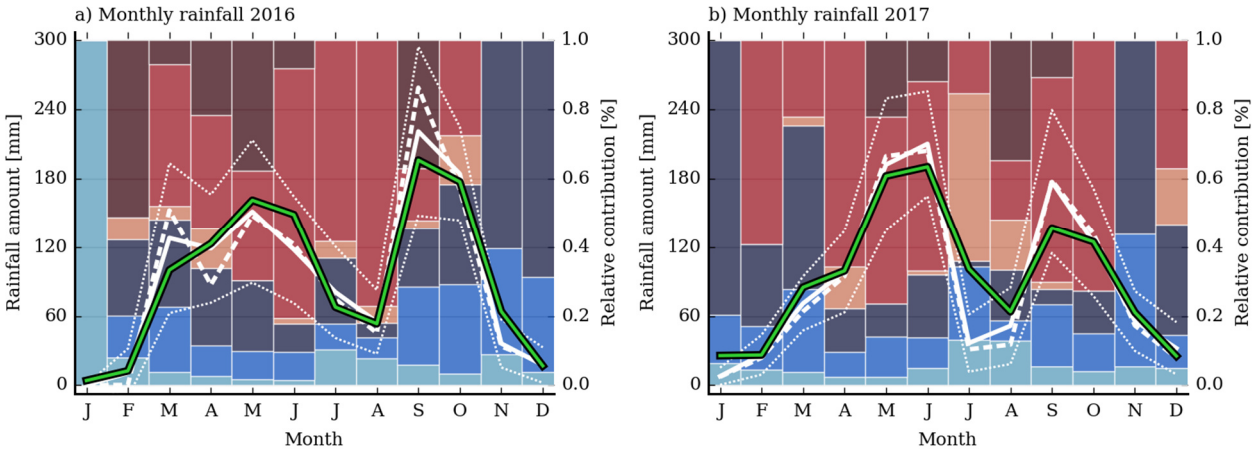

Figure 6: *Seasonal cycles of (a) 2016 and (b) 2017. The solid white line depicts the monthly rainfall averaged over all rain gauges with at least 90% of available data in a month. The dashed and thin dotted white lines are the monthly median and standard deviation around the mean (plus and minus 1 sigma). The solid green line is the monthly rainfall in IMERG averaged over all IMERG gridpoints collocated with the DACCIWA rain gauges. The coloured bars indicate the relative contribution to monthly rainfall by the defined rainfall types (see Fig. 5 for colour assignment).*

In the following, we make use of a contingency table (Table 1), which is a simple method that has been commonly used for model and forecast verification. A “hit” is registered wherever daily rainfall is greater than zero in both rain gauges and IMERG pixels. Accordingly, a “miss” (“false alarm”) refers to days where rainfall is registered in the rain gauges (IMERG) while absent in IMERG (rain gauges).

Table 1: *Contingency table. The colours refer to the figures in the following sub-sections.*

	IMERG yes	IMERG no
Rain gauge yes	**Hit**	**Miss**
Rain gauge no	**False alarm**	**Correct negative**

Figure 7 shows the variance of the daily rainfall difference between IMERG and the rain gauges as boxplots in each month and for each case of Table 1 (correct negatives are not considered since the rainfall is zero in both datasets). To begin with, the variation in daily rainfall difference is largest for “hits” and is of comparable magnitude in each month. While the median is close to zero, the boxes and whiskers for “hits” do not suggest a considerable bias as they do not extend preferably toward the positive or negative side. However, the daily rainfall difference can be as large as 12 mm in the interquartile range for “hits”. “False alarms” (“misses”) are positive (negative) by definition and do not exhibit the same magnitude in daily rainfall difference as for “hits”. This suggests that mostly weak rainfall events are missed or falsely detected by IMERG. However, as indicated by the curves in the lower part of Figure 7, IMERG is prone to false alarms (orange curve), which generally account for almost 50% of rainy days during the wet periods and rise to over 90% in the dry season month of January. The curve for hits is bimodal and reflects the seasonal cycle: the more rainy days there are, the higher the fraction of hits. Missed events are relatively rare, but interestingly increase during the months of July and August, which is the so-called little dry season (see also Figure 6). Overall, the hit rate on a daily basis is compromised by the frequently occurring false alarms, which appear to be a general problem within IMERG and which is not limited to specific months. But it becomes particularly visible in the dry period between November and February.

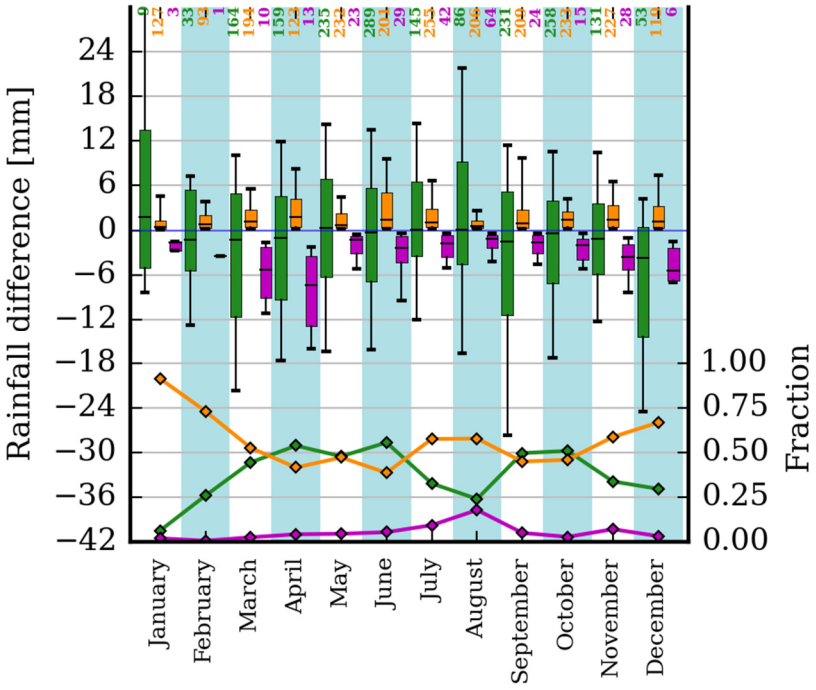

Figure 7: *Boxplots showing the variance of the daily rainfall difference between IMERG and rain gauges in the case of hits (green), false alarms (yellow) and missed events (purple) for each month (2016 and 2017 as well as all rain gauges are combined here). The boxes show the interquartile range with the median as a short horizontal black line, whereas the whiskers comprise the 10th and 90th percentile, respectively. The curves in the lower part of the panel indicate the relative frequency of each case based on every rainy day in both rain gauges and IMERG. The numbers at the top of the panel indicate the number of each case (colours as defined).*

3 Rainfall-type based validation of GPM IMERG at sub-daily time scales

3.1 Categorial validation

In this section, we exemplarily take rainfall types at the opposing end of the intensity-duration spectrum, weak short rainfall (WSR) and strong long rainfall (SLR), to analyse the performance of IMERG on a sub-daily basis. We note that the one-minute-based rain gauge dataset was aggregated to half-hourly rainfall for the purpose of comparability with IMERG. Similar to the previous section, the contingency table is used, however, with one minor change: A hit is assigned to IMERG as long as at least one half-hour interval overlaps with its counterpart in the rain gauge data. Longer or shorter event durations are neither false alarms nor misses.

Figure 8 shows the variance of rainfall difference integrated over the duration of WSR events between IMERG and the rain gauges. Since WSRs are identified through rain gauge data, false alarms are not considered here. Not surprisingly, missing WSRs lead to an overall small integrated rainfall difference. More interestingly, whenever WSR events are detected in IMERG, their rainfall amount is almost always overestimated with a maximum interquartile difference of 16 mm in July. The main reason is the overestimation of the event duration (not shown). However, the variation of rainfall difference itself changes over the course of the year, particularly evident for from July to August. Looking at the seasonal cycle of the frequency of missed events (purple curve in the bottom part of Figure 8), a pronounced peak during July and August becomes apparent. IMERG seemingly has difficulties to detect the WSRs during the little dry season. We note that this season is generally marked by a deep and moist boundary layer, which, however, is often capped by one or more stable and dry as well as moist and neutrally stratified layers aloft (see Figure 9). Consequentially, extensive periods of non-precipitating clouds at several tropospheric levels with rather low vertical extent are a typical feature of the little dry season. This may be an important error source for weak rainfall within IMERG. Outside of the little dry season, the miss rate is lower. However, we also note that only the nearest IMERG grid points to the rain gauges were evaluated. Adjacent pixels were not regarded.

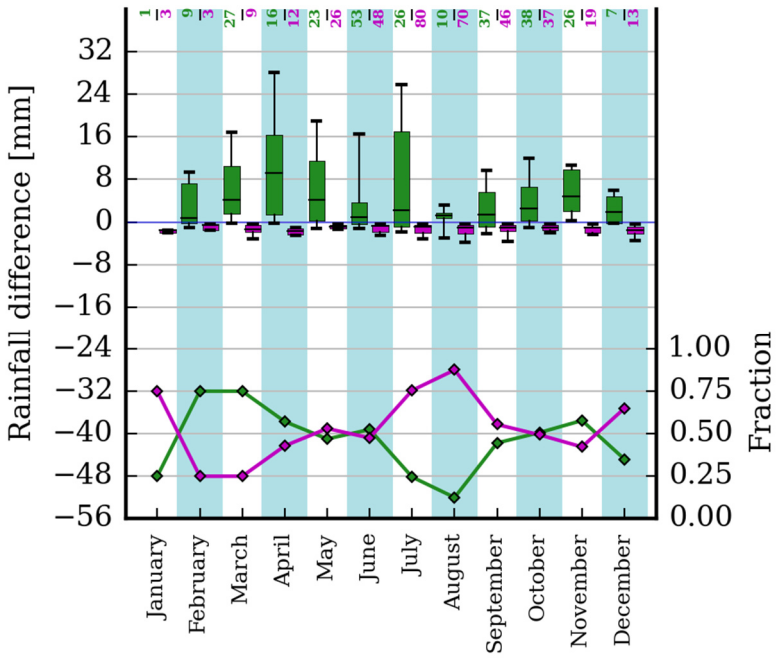

Figure 8: *Similar to Fig. 7, but on an event timescale for weak short rainfall (WSR) and solely based on rain gauge data. Because of the latter, no false alarms can occur.*

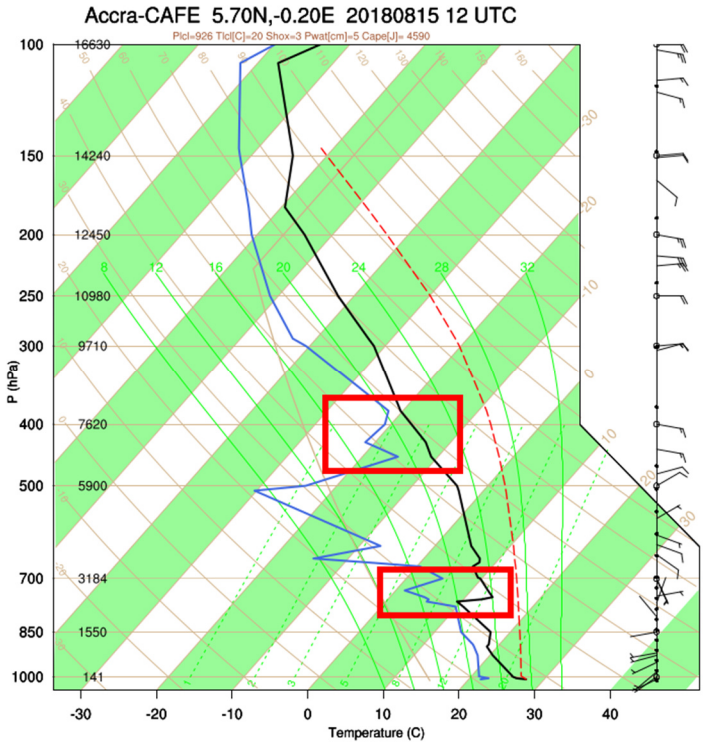

Figure 9: *Skew-T-log-p diagram of a radiosonde launch in Accra on 15 August, 2018, during the aircraft campaign "CAFÉ-Africa" (Chemistry of the Atmosphere – Field Experiment in Africa). The solid black and blue curves are the vertical profiles of ambient air temperature and dewpoint, respectively. The dashed red line denotes the temperature within a theoretical surface-based air parcel while being lifted upwards. The red boxes indicate layers potentially containing clouds, which enclose a deep dry layer.*

In Fig. 10, the same statistics are plotted for strong long rainfall (SLR) events, which, as mentioned earlier, are typically related to MCSs. Here, the box-whisker plots indicate similar characteristics as in Fig. 7, i.e. SLR events are not systematically over- or underestimated. The hit ratio is almost 100% in each month. It is promising to see that IMERG is able to capture these events both with respect to timing and position.

Summarising the results from the other rainfall types (not presented here), the miss rate is generally low if the event is high in intensity and/or the duration is long (i.e. LRs). However, IMERG tends to underestimate intense rainfall, which suggests that IMERG is at times unable to resolve the high intensity of the convective part of rainfall systems, which may occur very locally.

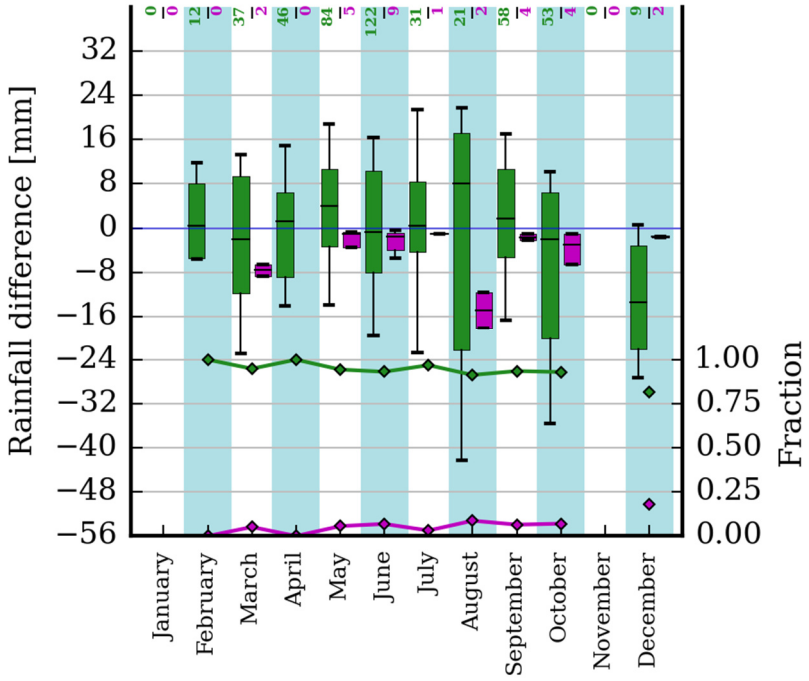

Figure 10: *Same as Fig. 8, but for strong long rainfall (SLR).*

3.2 Projection onto the seasonal cycle

With the information of hits, misses and false alarms gained in the previous sub-section, we are able to partition the seasonal cycle of IMERG based on the defined rainfall types. This is illustrated in Fig. 11. Similar to the rain gauges, the majority of rainfall within IMERG emerges from LRs (red bars), which can be largely attributed to overpassing MCSs. Shifting the attention to the orange bars, which quantify relative contribution of false alarms to total monthly rainfall in IMERG, it becomes apparent that over one fifth of IMERG rainfall comes from false alarms. Their contribution is generally highest in the dry months between November and February, but is also pronounced in July and August. The latter is more remarkable given the fact that the occurrence of missed events in these two months is highest in a relative sense (Fig. 7), particularly for WSRs (Fig. 8). In the same manner, the missed events and their sources are quantified and identified in Fig. 12. As previously mentioned, missed events are relatively rare. As such, the integrated rainfall amount (dashed purple curve) is relatively small. Most of the missed events emerge from the inability of IMERG to detect short rainfall (blue bars), at least at the rain-gauge-collocated grid points.

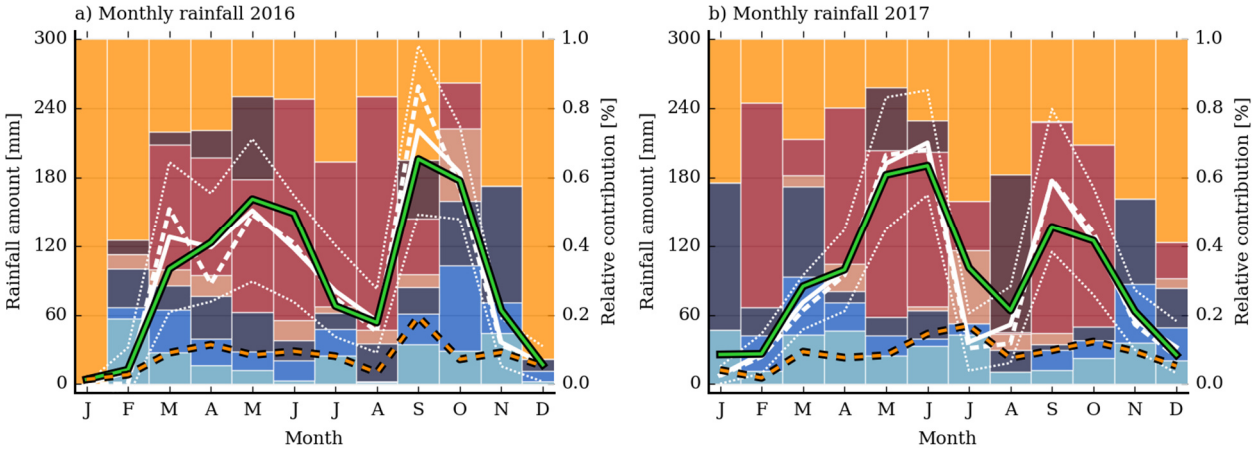

Figure 11: *Similar to Fig. 6, but the coloured bars refer to the monthly IMERG rainfall (solid green curve). Orange bars depict the contribution from false alarms. The dashed orange line indicates the integrated rainfall amount of false alarms.*

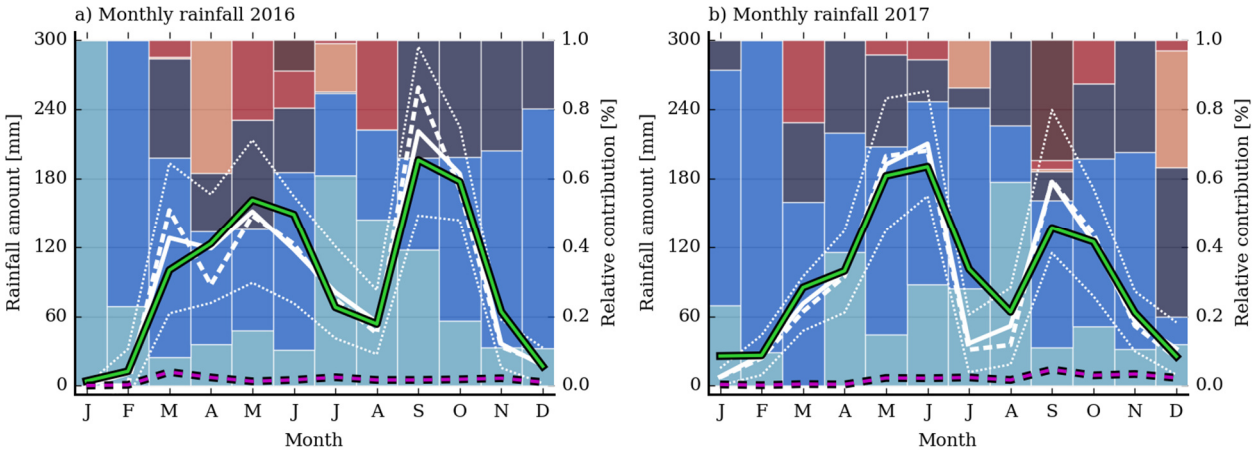

Figure 12: *Similar to Fig. 11, but the coloured bars indicate the relative contribution to the rainfall amount by missed events (dashed purple curve).*

3.3 Conclusion

The DACCIWA rain gauge network has been offering exciting and important opportunities to validate satellite rainfall in this complex moist tropical environment. Particularly the validation of the IMERG dataset with its high spatiotemporal resolution is of high interest since IMERG is anticipated to provide new insights into the variability of rainfall and their relationship to different types of rainfall systems. Herein, key findings on daily and sub-daily timescales are:

- Differences in daily rainfall amounts between IMERG and DACCIWA optical rain gauges highest during “hits”, however, with no obvious systematic error.
- Frequency of false alarms is relatively high. Of all rainy days within the rain gauges and IMERG, the false alarm rate ranges from 45% during the wet season to over 90% in the dry season. Although false alarms are largely weak rainfall events, they account of over one fifth of total rainfall within IMERG. However, their contribution is crucial to achieve a comparable monthly rainfall amount to the rain gauges during the rainy season.
- Missed events are relatively rare but peak during the little dry season in July and August, potentially because of the frequent occurrence of clouds at several tropospheric levels. Mostly short rainfall events, but particularly those of weak intensity are missed by IMERG.
- IMERG tends to overestimate the rainfall amount of weak and short rainfall events, but underestimate intense and/or long rainfall events, leading to a partial error compensation between different rainfall types.

In general, the present validation reveals an interesting behaviour of IMERG and adds an important perspective to the overall well-captured seasonal cycle of the rain gauges. While the monthly rainfall in IMERG is of similar magnitude to the rain gauges, some major differences were found with respect to the occurrence of rainfall events. Most notably, false alarms contribute strongly to monthly IMERG rainfall. Although individual false alarm events are usually not strong, they are frequent, particularly in the drier months of the West African monsoon. It remains to be analysed what the reasons for this is. The IMERG dataset largely contains rainfall estimates from infrared-based retrieval techniques, which is known to have deficiencies because of the indirect relationship between cloud-top temperature and rainfall intensity (Kidd et al., 2011). A cloud dataset such as CLAAS (CLoud property dAtAset using SEVIRI, Stengel et al., 2014) may help identifying certain cloud types that lead to the important source of error that false alarms are. The sketched avenue of further research is currenntly pursued and is planned to result in a publication (Maranan et al. 2019, in preparation).

As for the rain gauge network, their ability to monitor rainfall on a minutely basis has proven to be of a valuable source not only for simply quantifying rainfall, but also to validate and identify error sources in rainfall products such as IMERG. Furthermore, in a data-sparse region such as southern West Africa, these rainfall datasets provide important information about the dynamics of the West African monsoon circulation, which directly influences the formation of cloud and, eventually, precipitation. Therefore, we are planning to sustain the network beyond the end of the DACCIWA funding period.

4 References

Barrios, S., L. Bertinelli, and E. Strobl. "Trends in rainfall and economic growth in Africa: A neglected cause of the African growth tragedy." *The Review of Economics and Statistics* 92.2 (2010): 350-366.

Dezfuli, A. K., Ichoku, C. M., Huffman, G. J., Mohr, K. I., Selker, J. S., van de Giesen, N., ... & Annor, F. O. (2017). Validation of IMERG Precipitation in Africa. *Journal of Hydrometeorology*, *18*(10), 2817-2825.

Hou, Arthur Y., et al. "The global precipitation measurement mission." *Bulletin of the American Meteorological Society* 95.5 (2014): 701-722.

Huffman, George J., et al. "The TRMM multisatellite precipitation analysis (TMPA): Quasi-global, multiyear, combined-sensor precipitation estimates at fine scales." *Journal of hydrometeorology* 8.1 (2007): 38-55.

Huffman, G. J., Bolvin, D. T., & Nelkin, E. J. (2015a). Integrated Multi-satellitE Retrievals for GPM (IMERG) technical documentation. *NASA/GSFC Code*, *612*(2015), 47.

Huffman, George J., et al. "NASA global precipitation measurement (GPM) integrated multi-satellite retrievals for GPM (IMERG)." *Algorithm theoretical basis document, version* 4 (2015b): 30.

Kidd, Chris, and V. Levizzani. "Status of satellite precipitation retrievals." *Hydrology and Earth System Sciences* 15.4 (2011): 1109-1116.

Maranan, M. et al. ‘dacciwa_kumasi_raingauges’. SEDOO OMP. doi: 10.6096/baobab-dacciwa.1772, (2018).

Maranan, Marlon, Andreas H. Fink, and Peter Knippertz. "Rainfall types over southern West Africa: Objective identification, climatology and synoptic environment." *Quarterly Journal of the Royal Meteorological Society* 144.714 (2018): 1628-1648.

Stengel, M., et al. "CLAAS: the CM SAF cloud property data set using SEVIRI." *Atmospheric Chemistry and Physics* 14.8 (2014): 4297-4311.

Upton, Graham JG. "A correlation–regression method for tracking rainstorms using rain-gauge data." *Journal of Hydrology* 261.1-4 (2002): 60-73.

Yengoh, G. T., Armah, F. A., Onumah, E. E., & Odoi, J. O. (2010). Trends in agriculturally-relevant rainfall characteristics for small-scale agriculture in Northern Ghana. *Journal of Agricultural Science*, *2*(3), 3.